Journal of Zhejiang University-SCIENCE A

# Thin film bulk acoustic wave filters with ring-dot electrodes

Jing LIU, Jian-ke DU, Ji WANG, Jia-shi YANG

**Key words:** Piezoelectric; Thin film; Vibration; Resonator; Filter

Cite this as: Jing LIU, Jian-ke DU, Ji WANG, Jia-shi YANG, 2018. Thin film bulk acoustic wave filters with ring-dot electrodes. *Journal of Zhejiang University-SCIENCE A (Applied Physics & Engineering)*, 19(10):786-795. https://doi.org/10.1631/jzus.A1700396

# Application

| Comparison with SAW & Ceramics | | | |
|---|---|---|---|
| | FBAR | SAWs | ceramics |
| Frequency | 400 MHz to 10 GHz | 1 MHz to 2 GHz | 1 MHz to 10 GHz |
| Size | Semiconductor (acoustic) | Semiconductor (acoustic) | Quarter wave (electric) |
| Q | 1000 | 100s | 100s |
| Temp Co | 20 to 30 ppm/C | 35 to 90 ppm/C | 0 to 5 ppm/C |
| Power | > 1 W | < 1W | >>1 W |

Table 1: AVAGO FBAR comparison with SAW and Ceramics

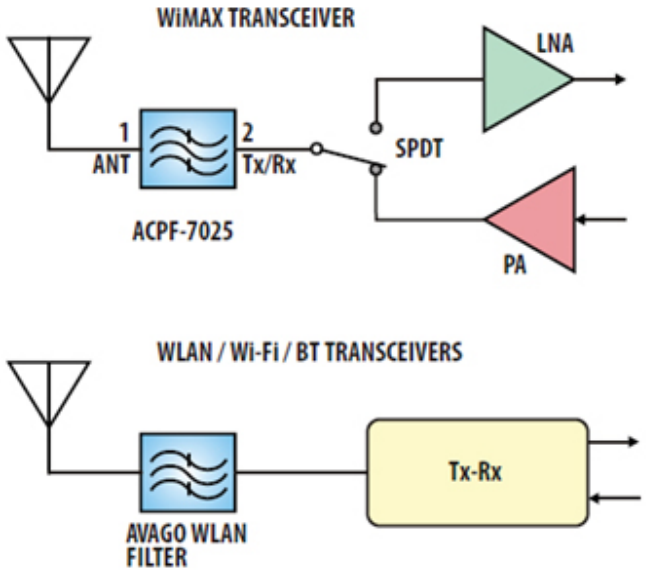


Figure 1: Typical multi system block diagram

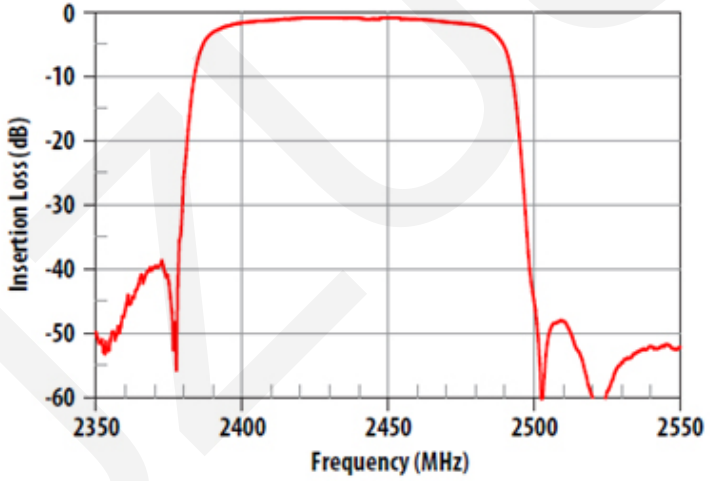


Figure 2: ACPF-7024 out of band attenuation 2350-2550MHz

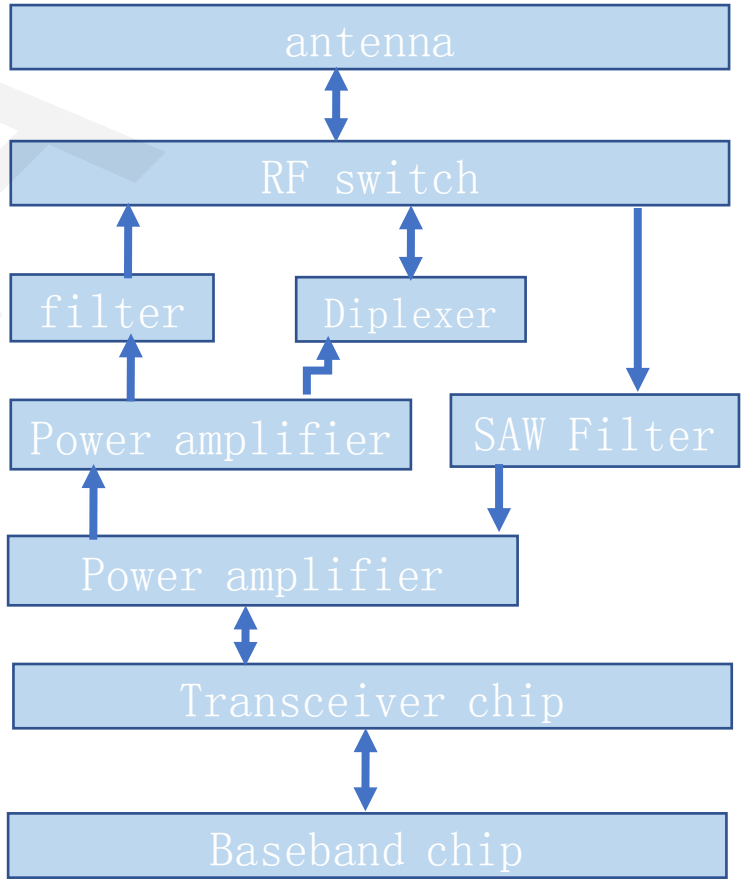


Figure 3: Filters play an important Role in RF front-end

# Governing Equation

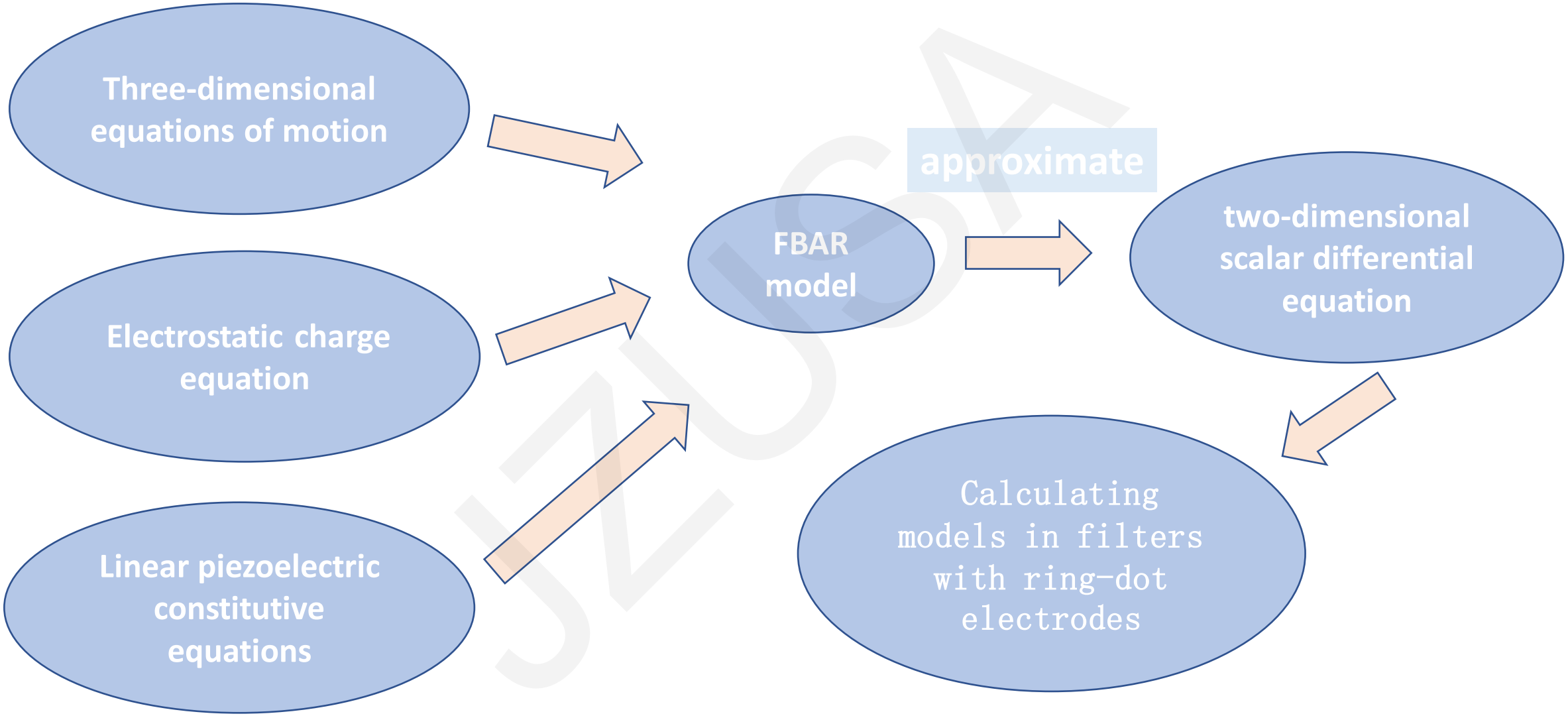

# Scalar Equations

## Mechanics Model

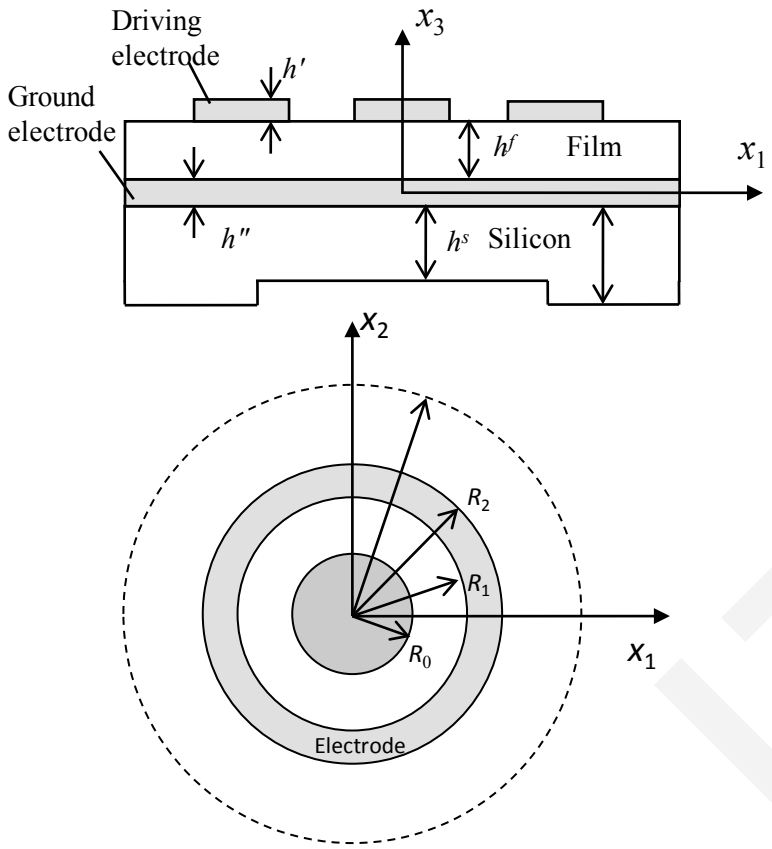


Figure 4: The lateral view and top view of a thin film bulk acoustic wave filter with ring-dot electrodes

## Tiersten-Stevens two-dimensional scalar differential equation:

$$M_n\left(\frac{\partial^2 u_3^{f^n}}{\partial x_1^2}+\frac{\partial^2 u_3^{f^n}}{\partial x_2^2}\right)-\bar{c}_{33}^f\tilde{\eta}_{f^n}^2 u_3^{f^n}-\rho^f\ddot{u}_3^{f^n}=0,$$

$$0<x_3<h^f.$$

$$M_n\left(\frac{\partial^2 u_3^{s^n}}{\partial x_1^2}+\frac{\partial^2 u_3^{s^n}}{\partial x_2^2}\right)-\bar{c}_{33}^f\tilde{\eta}_{f^n}^2 u_3^{s^n}-\rho^f\ddot{u}_3^{s^n}=0,$$

$$0>x_3>-h^s.$$

$$u_3^{f^n}=\left(A_3^{s1n}\cos\eta_{s^n}^0 x_3+B_3^{s1n}\sin\eta_{s^n}^0 x_3\right)f^n(x_1,x_2,t),$$

$$0>x_3>-h^s.$$

$$u_3^{f^n}=\left(A_3^{f1n}\cos\eta_{f^n}^0 x_3+B_3^{f1n}\sin\eta_{f^n}^0 x_3\right)f^n(x_1,x_2,t),$$

$$0<x_3<h^f.$$

# Numerical Results

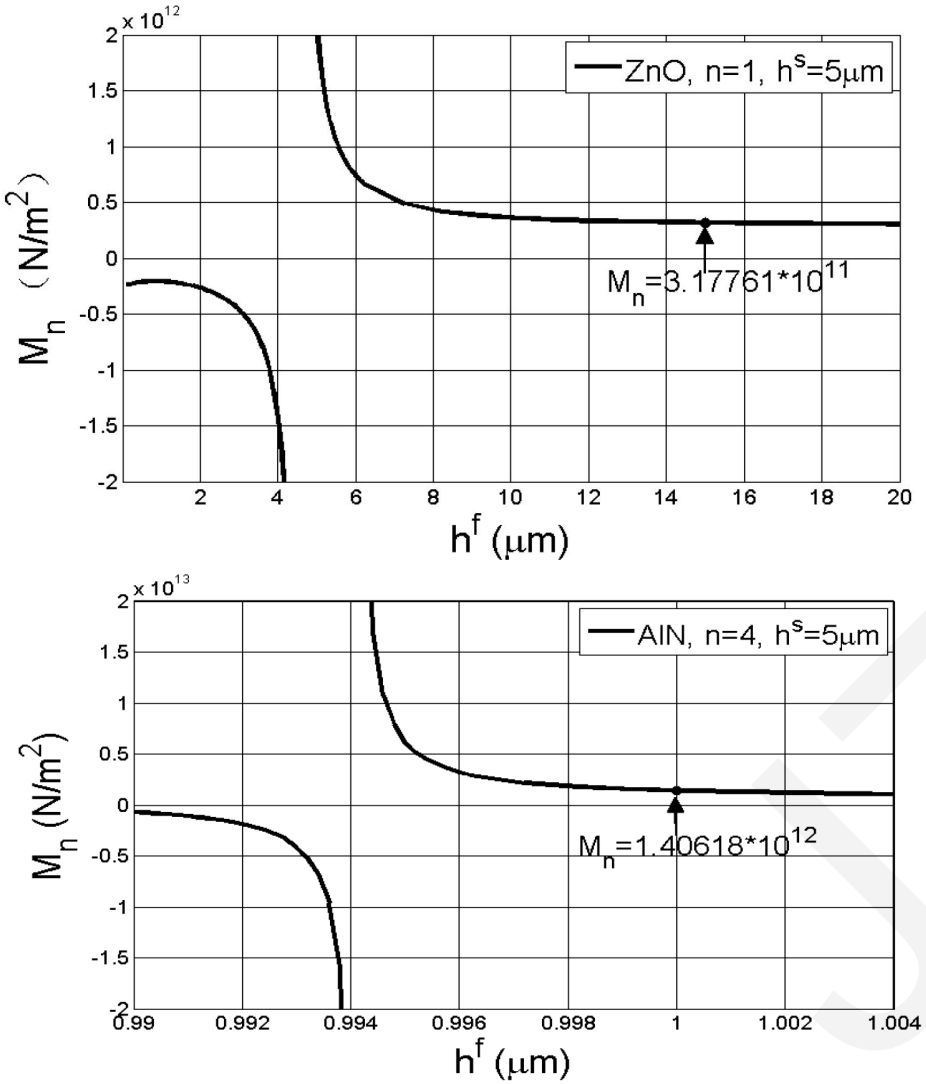


Figure 5: Mn for (a) ZnO on Si with *n*=1, and (b) AlN on Si with *n*=4.

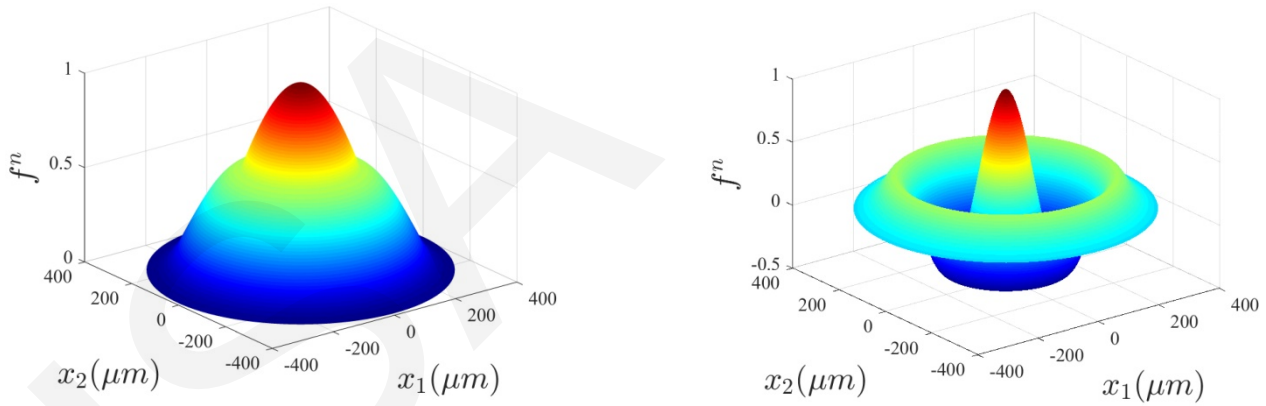


Figure 6: Two trapped thickness-extensional modes. (a) $f_1$=365.5336 MHz (b) $f_2$=367.4778 MHz

| $R_0$ (μm) | $R_1$ (μm) | $R_2$ (μm) | $h'$ (μm) | $\rho'$ (g/m$^3$) | $(f_1+f_2)/2$ (MHz) | $f_2-f_1$ (kHz) |
|---|---|---|---|---|---|---|
| 150 | 160 | 320 | 0.044 | 19.3 | 366.5057 | 1944.2528 |
| 130 | 160 | 320 | 0.044 | 19.3 | 366.8929 | 1331.3685 |
| 120 | 160 | 320 | 0.044 | 19.3 | 367.0877 | 1260.6349 |
| 150 | 170 | 320 | 0.044 | 19.3 | 366.6965 | 1600.5770 |
| 150 | 180 | 320 | 0.044 | 19.3 | 366.8634 | 1402.4924 |
| 150 | 160 | 350 | 0.044 | 19.3 | 366.2283 | 1641.4400 |
| 150 | 160 | 400 | 0.044 | 19.3 | 365.9003 | 1349.9358 |
| 150 | 160 | 320 | 0.200 | 19.3 | 349.6776 | 1718.8152 |
| 150 | 160 | 320 | 0.400 | 19.3 | 327.9103 | 1534.1840 |
| 150 | 160 | 320 | 0.044 | 10.2 | 368.7126 | 1959.9168 |
| 150 | 160 | 320 | 0.044 | 2.7 | 370.5160 | 1956.7986 |

Table 2 Average frequency and frequency difference of the operating modes

# Conclusions

- Within the narrow frequency interval , there exist a few trapped modes with vibrations mainly under the dot-ring electrodes.
- With proper design, the nodal line of the second trapped mode lies in the gap between the ring and the dot electrodes. Then the first two trapped modes of the proposed structure can be used as the ideal operating modes for a filter.
- The location of the nodal line and the decay rate of the fields away from the electrode edges are sensitive to geometric and physical parameters.